View Article Online / Journal Homepage / Table of Contents for this issue

PAPER

NJC
www.rsc.org/njc

Weak interactions between resorcinarenes and diquaternary alkyl ammonium cations

Heidi Mansikkamäki,[a] Christoph A. Schalley,[b] Maija Nissinen[a] and Kari Rissanen*[a]

[a] *Nanoscience Centre, University of Jyväskylä, P.O. Box 35, FIN-40014 Jyväskylä, Finland. E-mail: hemansik@cc.jyu.fi, majoni@cc.jyu.fi, kari.rissanen@jyu.fi; Fax: +358 14 260 2501; Tel: +358 14 260 2672*

[b] *Kekulé-Institut für Organische Chemie und Biochemie der Universität, Gerhard-Domagk-Str. 1, D-53121 Bonn, Germany. E-mail: c.schalley@uni-bonn.de*

Received (in Montpellier, France) 1st October 2004, Accepted 5th November 2004
First published as an Advance Article on the web 9th December 2004

Published on 09 December 2004 on http://pubs.rsc.org | doi:10.1039/B415401K
Downloaded on 01 January 2013

The interactions of resorcin[4]arenes **1** with alkyl ammonium cations bearing a 1,4-diazabicyclo[2.2.2]octane (DABCO) scaffold ($\mathbf{3}^{2+}$, $\mathbf{4}^{2+}$ and $\mathbf{5}^{2+}$) were analyzed in the solid state by X-ray crystallography, in solution by ^{1}H NMR spectroscopy, and in the gas phase by ESI-TOF mass spectrometry. The results are complemented with AM1 calculations and compared to previous reports on complexation studies of resorcinarenes with quaternary alkyl ammonium cations. The NMR titration results indicate that there are hardly any differences in the binding of the quaternary tetramethyl ammonium cation $\mathbf{2}^+$ and the diquaternary *N*,*N*'-dimethyl DABCO dication $\mathbf{4}^{2+}$. The large *N*,*N*'-dibenzyl DABCO dication $\mathbf{5}^{2+}$ has two potential sites for inclusion, that is, the aryl groups and the central cationic part, and the complexation and interactions of both sites with **1** were verified in the NMR studies as well as in the solid state structures.

Introduction

Self-assembling, reversibly hydrogen-bonded capsules[1] have contributed a great deal to our current understanding of enzyme action. The size-selective,[2] and in some cases even stereoselective,[3] inclusion of suitable guest molecules and the possibility to accelerate or catalyze chemical reactions[4] within such capsules provide profound and general insights into the particular properties that govern the substrate specificity and the rate enhancement observed in biocatalysts.

One family among these capsules is based on calixarenes or resorcinarenes (*e.g*, **1a–1f**, Scheme 1). They have attracted great interest in supramolecular chemistry as models for receptors[5] and as building blocks in various frameworks ranging from molecular capsules[6] to tubular assemblies.[7] The well-known solvent-assisted hexameric capsule of *C*-methyl resorcinarene, encapsulating neutral solvent molecules, is no doubt one of the most fascinating solid state resorcinarene assemblies.[8] Several studies have shown that lipophilic resorcinarenes, (*e.g*, **1f**) assemble into a hexameric capsule in water-saturated benzene and chloroform.[9]

There are several studies on the dimeric analogues of hexamer capsules.[6] Dimeric capsules that are solvent-mediated, like the hexamer capsule in the solid state, have been shown to encapsulate both neutral solvent molecules[6b] and small alkyl ammonium cations.[6a,c–f] Resorcinarenes have quite a high affinity towards alkyl ammonium cations in alkaline solution due to the deprotonation of the resorcinarene host and the resulting electrostatic interactions between host and guest.[10a] Under neutral conditions, closer to the biological environment, the binding of quaternary alkyl ammonium cations is weakened by a factor of several hundreds compared to the binding constants observed in alkaline solutions.[10a] Even though these results point towards rather weak cation-π interactions, these noncovalent forces are sufficiently high to act as a significant driving force in biological processes such as protein folding.[11] Therefore, a better understanding of the subtle details related to them is an important research topic.

Besides crystallography and solution-phase studies of the binding interactions of cations to resorcinarenes, mass spectrometry[12] is a perfectly suited tool for their examination, because it makes advantageous use of the cation present in the complex and gives access to data from the gas phase.[13] Dimeric capsules of resorcinarenes and related compounds encapsulating small cations have been shown to prevail in the gas phase without solvent mediation and have been predicted to be directly hydrogen bonded.[14]

In this report, interactions of doubly protonated and *N*,*N*'-bisalkylated DABCO derivative cations $\mathbf{3}^+$–$\mathbf{5}^+$ with resorcinarenes **1b–1f** are analyzed, starting with the solid state structures of their corresponding complexes, followed by an NMR investigation of their interactions in solution, and finally, a discussion on the inclusion properties of diquaternary alkyl ammonium cations in the gas phase. The results are

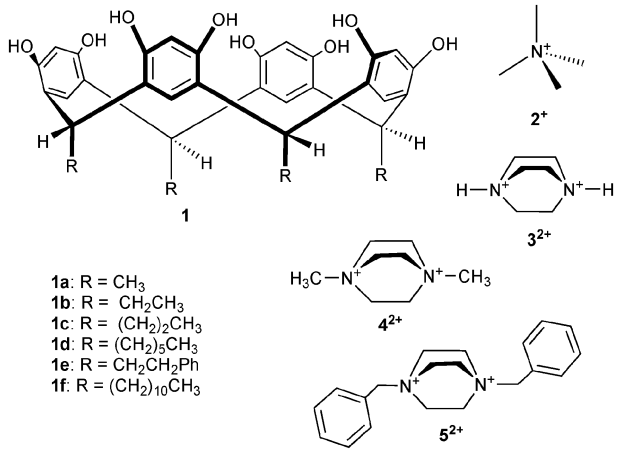

Scheme 1

DOI: 10.1039/b415401k

This journal is © The Royal Society of Chemistry and the Centre National de la Recherche Scientifique 2005

View Article Online

compared to earlier reports of resorcinarene complexes with quaternary and diquaternary alkyl ammonium cations.[6e,f,10a]

Results and discussion

Single-crystal X-ray analysis

In the following section, seven novel crystal structures of ammonium ion complexes of resorcinarenes **1b–1f** are reported: one complex with tetramethyl ammonium $\mathbf{2}^{+}$, four complexes with *N*,*N*′-dimethyl DABCO $\mathbf{4}^{2+}$ and two complexes with *N*,*N*′-dibenzyl DABCO $\mathbf{5}^{2+}$.

Complexes of quaternary cations. Complexation of resorcinarenes **1a–1c** and small quaternary alkyl ammonium salts, such as $\mathbf{2}^{+}$ or dimethyl diethyl ammonium cation, results in dimeric solvent-mediated hydrogen-bonded capsules, when crystallized from relatively hydrophilic solvents such as alcohols, as we previously observed.[6e]

We performed similar crystallization experiments with **1d** and **1f**, but, so far, we have not been able to co-crystallize quaternary alkyl ammonium cations with these two resorcinarenes. Instead of the complexation of the cation, solvent inclusion was observed or there simply were no crystals suitable for X-ray measurement.

On the contrary, crystallization of **1e** with $\mathbf{2}^{+}Br^{-}$ (Me_4NBr) from aqueous MeOH produces a dimeric solvent- and bromide-mediated capsule, complex **I** (**1e** · 0.5 $\mathbf{2}^{+}$ · Br^{-} · 2.5 MeOH · 0.5 H_2O, Fig. 1). The asymmetric unit comprises half a capsule, that is, one resorcinarene, which is in an almost perfect crown conformation (distances between centroids of opposite aromatic groups are 6.8 and 7.0 Å), stabilized by four intramolecular hydrogen bonds between the phenolic hydroxyl groups. The encapsulated cation $\mathbf{2}^{+}$ is severely disordered, as are also the co-crystallized methanol molecules and the bromide. Due to the disorder of the capsule-mediating solvents and anions, the hydrogen-bonding scheme and the interactions holding the two halves together are difficult to analyze. However, it is justified to say that this capsule is not fully bound together as were our previous capsules,[6e,f] since all of the solvents hydrogen bonded to the hydroxy groups of **1d** are not linked to both of the capsule halves *via* H-bonds, *i.e.* they do not play a mediating role in capsule formation. The capsules pack further to form hydrogen-bonded ribbons where the dimers of **1e** are mediated by the bromide anions [Fig. 1(b) and 1(c)].

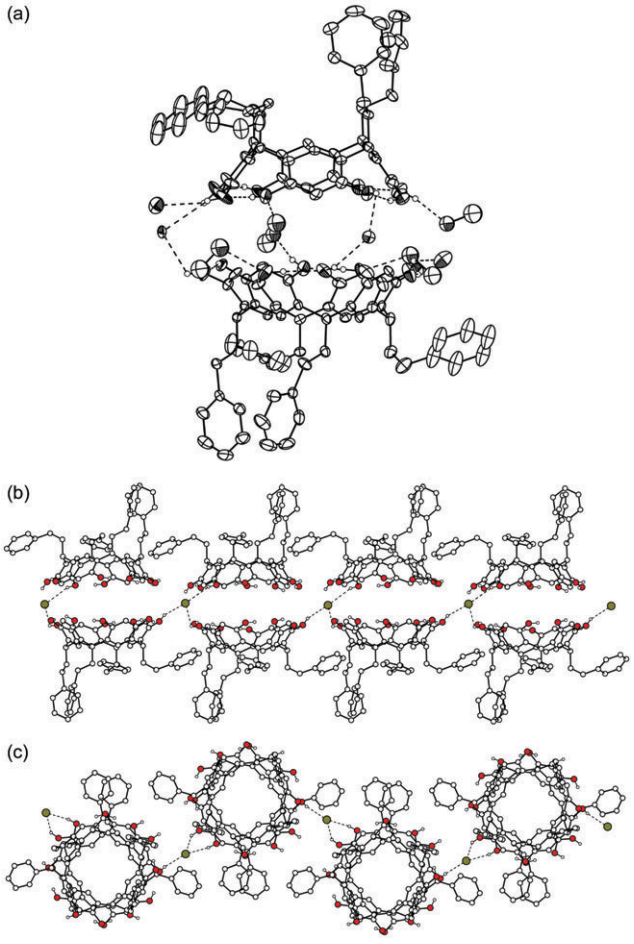

Fig. 1 X-Ray crystal structure of complex **I**. (a) A thermal ellipsoid (30% probability level) illustration of the dimeric capsule of **1e**. Hydrogen bonds are indicated by dashed lines. Only OH hydrogens are shown. The other hydrogens, as well as the disordered cation and solvent molecules, are omitted for clarity. (b) Packing view showing the hydrogen-bond linkage of adjacent capsules. The cations, hydrogen atoms and solvent molecules are omitted. (c) Top view of the capsule chain.

Complexes of protonated DABCO,[6f] $\mathbf{3}^{2+}$. Despite several crystallization attempts of $\mathbf{3}^{2+}$ complexes with **1b–1f** in various solvents (MeOH, EtOH, *n*-propanol, acetonitrile and their mixtures) and with various counteranions (Cl^{-}, Br^{-}, I^{-}, PF_6^{-}, BF_4^{-}), only one solid-state complex of $\mathbf{3}^{2+}$ with **1b** could be obtained. Like the complexes with small quaternary cations, this complex is also a dimeric capsule.[6f] It is noteworthy that the cation is severely disordered, which, together with the lack of formation of other crystalline structures, indicates that there is a very small binding affinity and that interactions between guest and host are not very specific or particularly strong.

Complexes of methylated DABCO, $\mathbf{4}^{2+}$. While capsule formation of **1** with $\mathbf{2}^{+}$ seems favourable when compared to other possible structures, $\mathbf{4}^{2+}$ as a guest molecule seems to be at the borderline, as far as the maximum guest size is concerned. In our previous studies, we have been able to crystallize one methanol- and water-extended capsule of **1b** enclosing the disordered $\mathbf{4}^{2+}$.[6e] To our knowledge, this is the only dimeric capsule structure obtained with this dication so far, which makes it a special case.

Instead of dimeric capsule structures, crystals of open complexes of **1** with both the chloride and the bromide salts of $\mathbf{4}^{2+}$ are easily obtained by slow evaporation from alcohol solutions. Here, we report four structures of such complexes: complex **II** (**1b** · 2 $\mathbf{4}^{2+}$ · 4 Br^{-} · *n*-PrOH · 2 H_2O), complex **III** (**1b** · $\mathbf{4}^{2+}$ · 2 Br^{-} · EtOH), complex **IV** (**1c** · $\mathbf{4}^{2+}$ · 2 Cl^{-} · 2 MeOH) and complex **V** (**1d** · 1.5 $\mathbf{4}^{2+}$ · 3 Br^{-} · EtOH · H_2O). The asymmetric unit of complex **II** comprises one resorcinarene (**1b**) and two $\mathbf{4}^{2+}$ cations with their bromide counterions, together with two water molecules and one *n*-propanol molecule [Fig. 2(a)]. One of the two cations is complexed within the cavity of **1b**, practically in a horizontal position, forcing **1b** to adopt a somewhat flattened crown conformation (distances of the centroids of the opposite aromatic rings are 6.6 and 7.2 Å). The other cation is located outside the resorcinarene cavity, interacting mostly with the counterions [Fig. 2(c)]. The shortest distances between the cation carbons and the centres of the closest aromatic rings of **1b** are 3.4 Å for CH_2, 3.6 Å for CH_3 and 4.4 Å for N^{+}, indicating C–H···π and N^{+}···π interactions. The $\mathbf{4}^{2+}$ dication is not located as deeply in the cavity as $\mathbf{2}^{+}$ in complex **I**, since the closest distance between the cation carbon and the plane formed by the methine bridges in **1b** is 3.6 Å for complex **I** and 4.4 Å for complex **II**. In the crystal packing hydrophobic and hydrophilic layers are formed [Fig. 2(c)], similarly to what is observed in the crystal structures of various other resorcinarene complexes.[6,15]

Crystallization of **1b** from aqueous ethanol with $\mathbf{4}^{2+}$ dibromide results in crystals of an open 1 : 1 complex **III** [**1b** · $\mathbf{4}^{2+}$ ·

Published on 09 December 2004 on http://pubs.rsc.org | doi:10.1039/B415401K
Downloaded on 01 January 2013

View Article Online

Published on 09 December 2004 on http://pubs.rsc.org | doi:10.1039/B415401K
Downloaded on 01 January 2013

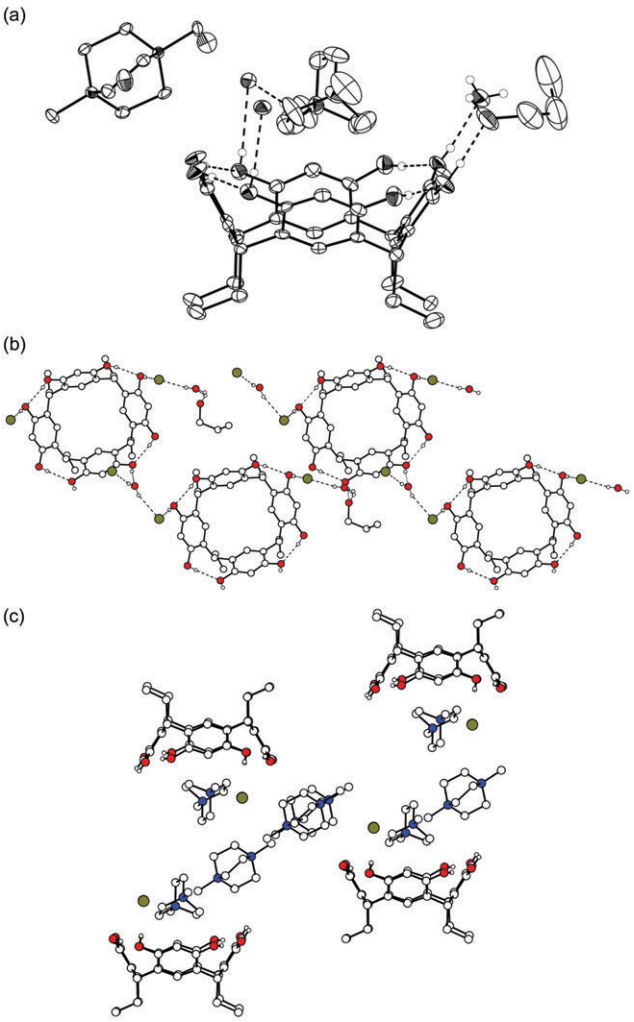

Fig. 2 X-Ray crystal structure of complex **II**. Non-hydrogen bonding hydrogen atoms are omitted for clarity. (a) A thermal ellipsoid (50% probability level) illustration of the asymmetric unit. One of the two bromide anions and one *n*-propanol solvent are H-bonded to hydroxyl groups. Hydrogen bonds are shown by dashed lines. (b) Molecules of **1b** are hydrogen-bonded to adjacent host molecules *via* H-bonds with *n*-propanol molecules or bromide anions. Cations are omitted for clarity. (c) Side view of the packing with guest ions, non-hydrogen bonding hydrogen atoms and solvent molecules omitted for clarity.

$2\,Br^- \cdot EtOH$, Fig. 3(a)]. Again, the co-crystallized EtOH solvent molecule and the bromide anions are hydrogen-bonded to **1b**, while the $\mathbf{4}^{2+}$ cation is located inside the slightly distorted **1b** with distances between centres of facing aromatic rings being 6.5 and 7.2 Å. In this case, the cation is in an upright position, slightly tipped away from the symmetry axis of **1b** to allow better interaction between the methyl group of the cation and an aromatic ring of **1b**. The shortest distances between CH_3, CH_2 and N^+ and the closest aromatic ring are 3.5, 3.3 and 3.9 Å, respectively. The upright position allows the cation to dive more deeply into the cavity with a distance of 2.8 Å between the closest guest's methyl carbon and the methine plane in **1b**, 0.8 Å shorter than the corresponding value for $\mathbf{2}^+$ in complex **I**. Each **1b** molecule is hydrogen-bonded to the adjacent **1b** *via* EtOH molecules and/or Br^- anions. The structure forms a wave-like H-bonded chain and hydrophilic and hydrophobic areas are layered [Fig. 3(b)].

Complex **IV** ($\mathbf{1c} \cdot \mathbf{4}^{2+} \cdot 2\,Cl^- \cdot 2\,MeOH$) resulted from crystallizing **1c** with $\mathbf{4}^{2+}$ dichloride in aqueous methanol (Fig. 4). It closely resembles complex **III** with respect to the cation binding and cation positions relative to the host. Also, the interactions of the chloride anions and MeOH solvent molecules with the upper rim OH groups of **1c** are similar. Adjacent resorcinarenes are also H-bonded to each other similarly, that is, they are mediated *via* hydrogen bonds to Cl^- and to methanol molecules.

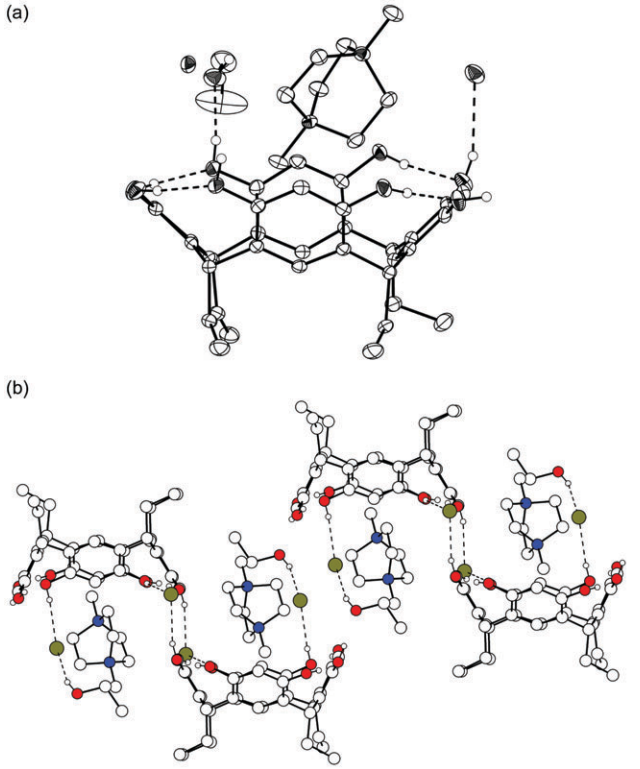

Fig. 3 X-Ray crystal structure of complex **III**. Non-hydrogen bonding hydrogens are omitted for clarity. Hydrogen bonds are shown by dashed lines. (a) A thermal ellipsoid (50% probability level) plot of the asymmetric unit. One of the two bromide anions and one EtOH are H-bonded to **1b**. (b) Resorcinarenes are connected *via* hydrogen bonds from phenolic OH groups to EtOH molecules, bromide anions and finally adjacent resorcinarenes, forming infinite chains.

It is interesting to compare the only dimeric capsule encapsulating $\mathbf{4}^{2+}$ (*i.e.*, a dimer of $\mathbf{1b}^{6f}$) with complex **IV** because its components differ only by the counteranion, which is a bromide instead of a chloride, and the host, which is **1b** instead of **1c**. The hydrogen-bonding scheme of the closed **1b** capsule is symmetrical and involves two water molecules in every other solvent bridge and one methanol molecule in every other bridge (Fig. 5). The cation position is horizontal and it is disordered over two positions with equal population parameters so that the methyl groups point into the corners of the hydrogen-bonding seam. This arrangement provides a good and tight fit for the dication inside the extended capsule's cavity (Fig. 5). Since the solvent system in both crystallization experiments was the same, it seems that the anion plays a pivotal role. In the capsular structure, the Br^- anions are located in-between the ethyl chains of the host, fairly far away from their counterions (7.9 Å), while in complex **IV**, the Cl^- ions are hydrogen-bonded to **1c** and located directly next to the cations [4.4 Å, Fig. 4(a)]. Since Cl^- is a harder anion than Br^-, and thus a better hydrogen-bond acceptor, it is hydrogen-bonded to the OH groups of the host. In contrast, the softer Br^- prefers the more lipophilic environment between the ethyl side chains. Also, the energy required for the charge separation of cation and anion is larger for Cl^-, favouring anion binding in the direct proximity of the cation.

Finally, as the last complex of *N*,*N*′-dimethylated DABCO, complex **V** ($\mathbf{1d} \cdot 1.5\,\mathbf{4}^{2+} \cdot 3\,Br^- \cdot EtOH \cdot H_2O$) was obtained by slow crystallization from aqueous ethanol. **V** is similar to complex **II** in the sense that there are two cations in different environments and only one of them is complexed inside the resorcinarene bowl, and this in a similar horizontal position as

View Article Online

Published on 09 December 2004 on http://pubs.rsc.org | doi:10.1039/B415401K
Downloaded on 01 January 2013

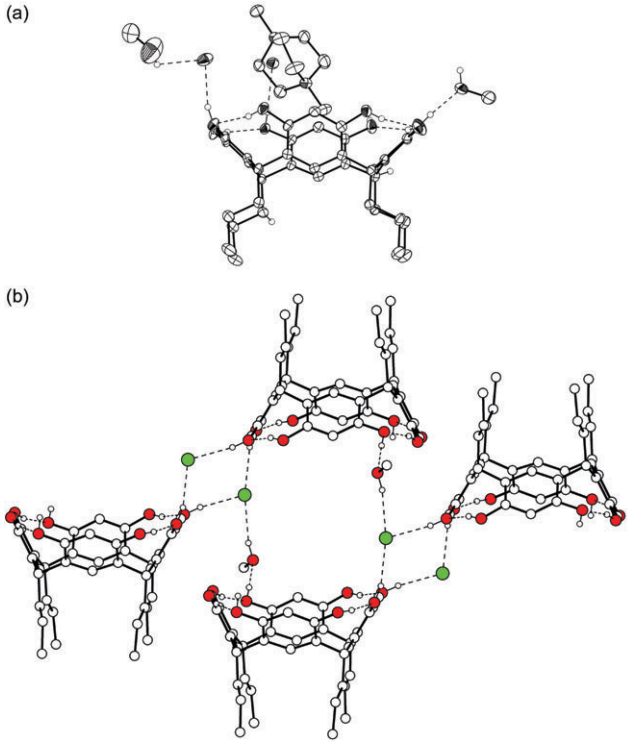

Fig. 4 X-Ray crystal structure of complex **IV** with hydrogen bonds shown by dashed lines. (a) Thermal ellipsoids with 50% probability. (b) Packing and H-bond network in the complex. The Br^- anions and one methanol molecule mediate the H-bonds between the hosts.

in complex **II** (Fig. 6). The other cation is part of a hydrophilic salt layer stabilized by electrostatic interactions. As typically observed with long alkyl chain resorcinarenes,[16] the hexyl chains of one layer are staggered with chains from adjacent layers. Thus, hydrophilic and hydrophobic layers are formed [Fig. 6(b)]. Two of the three bromide anions in the asymmetric unit are disordered over two positions, which makes a detailed study of the hydrogen bonding basically impossible. The **1d** molecules are directly hydrogen-bonded to two other **1d** molecules and are additionally indirectly bridged by hydrogen bonds between a bromide anion and two OH groups of the adjacent resorcinarenes [Fig. 6(c)]. Three intramolecular hydrogen bonds stabilize the clearly flattened crown conformation of **1d** (distances between centroids of opposite aromatic groups are 6.4 and 7.4 Å). This distortion of the **1d** bowl and the fact that only one of the three DABCO bridges is complexed in the bowl (instead of two of them as in complex **II**) allows the dication $\mathbf{4}^{2+}$ to come a little closer to the aromatic groups of the host (closest distances for CH_2, CH_3 and N^+ are

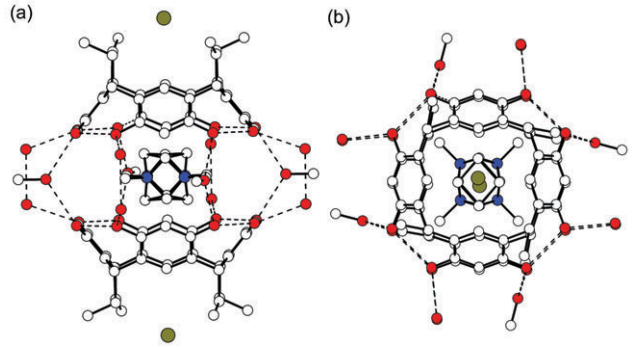

Fig. 5 X-Ray crystal structure of the dimeric **1b** capsule encapsulating disordered $\mathbf{4}^{2+}$. (a) Side view of the capsule showing the hydrogen-bonding pattern with dashed lines. The bromide anion is located in between the ethyl chains of **1b**. (b) Top view of the capsule. Hydrogens are omitted for clarity.[6f]

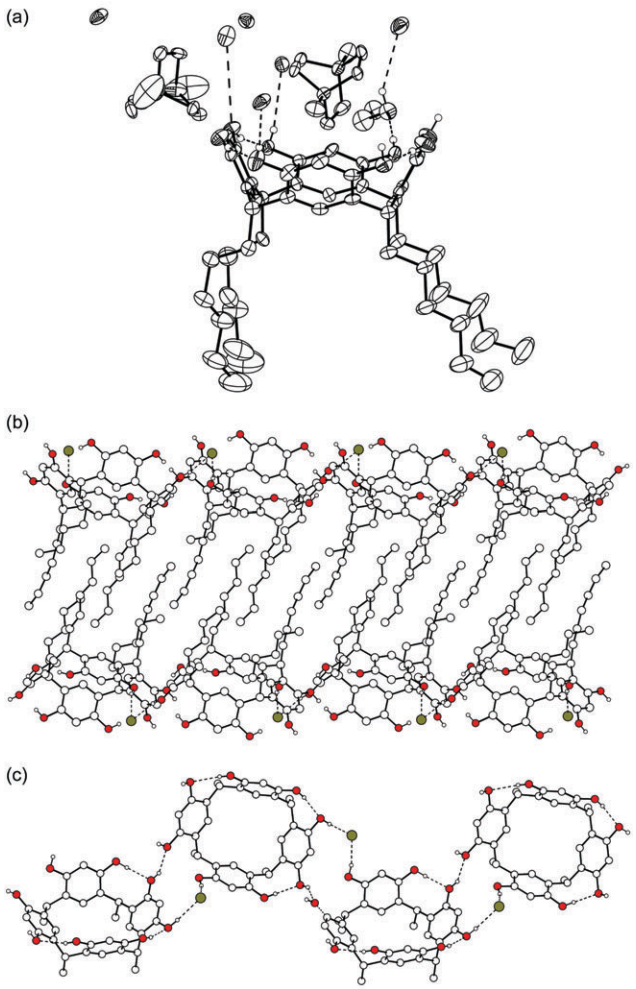

Fig. 6 X-Ray crystal structure of complex **V**, where only OH hydrogens are shown. (a) Thermal ellipsoid plot of the complex. (b) The alkyl chains of **1d** stagger together forming hydrophilic and hydrophobic layers. (c) Hydrogen bonds connect adjacent **1d** molecules. Cations and solvent molecules are omitted for clarity.

3.3, 3.4 and 4.3 Å, respectively) and to the plane of the methine bridges of **1d** (3.5, 3.8 and 4.2 Å for CH_2, CH_3, and N^+, respectively).

Salts of poor hydrogen bond acceptors such as I^-, PF_6^- and BF_4^- were used in crystallization experiments, but, so far, no suitable crystals were obtained for analysis. The co-crystallization of **1f** with $\mathbf{4}^{2+}$ halide salts from ethanol resulted only in crystals of the known ethanol solvate of **1f**.[16] This effect was also observed with methanol.

Complexes of bisbenzylated DABCO $\mathbf{5}^{2+}$. Complexation of bisbenzylated DABCO salts attracted our interest due to its two competing binding sites with resorcinarenes. In addition to the DABCO moiety, the aromatic benzyl groups in $\mathbf{5}^{2+}$ are potential guests, with their ability to interact by $\pi\cdots\pi$ interactions as shown in studies with planar aromatic guests.[17]

Two solid state structures, complex **VI** ($2\,\mathbf{1c}\cdot 1.5\,\mathbf{5}^{2+}\cdot 3\,Br^-\cdot 0.5\,H_2O\cdot 7\,MeOH$) and complex **VII** ($\mathbf{1f}\cdot 0.5\,\mathbf{5}^{2+}\cdot Br^-\cdot 2.5\,EtOH$), provide examples of the two competing binding modes. In complex **VI**, which was crystallized from methanol, two independent resorcinarenes and two dications with different environments are found. One of the cations clearly interacts with a **1c** molecule and is complexed with the DABCO moiety in a horizontal position, similarly to complexes **II** and **V**. The two benzyl groups point away from the resorcinarene [Fig. 7(a)]. The resorcinarene again adopts a flattened crown conformation (distances between the opposite aromatic groups

View Article Online

Published on 09 December 2004 on http://pubs.rsc.org | doi:10.1039/B415401K
Downloaded on 01 January 2013

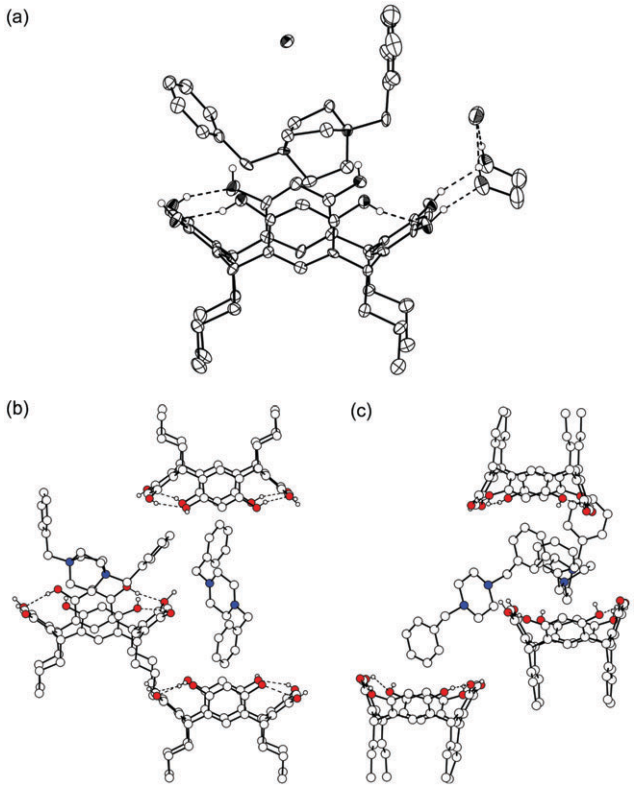

Fig. 7 X-Ray crystal structure of complex **VI**. (a) Thermal ellipsoid plot drawn with 50% probability level of one of the cations and resorcinarenes in the structure. (b) View of the second, disordered dication and its interactions with **1c** molecules. (c) Side view of the arrangement.

are 6.3 and 7.5 Å), held together *via* intramolecular H-bonds, while the remaining OH groups are hydrogen-bonded to methanol and disordered water molecules or to the bromide anions. The other cation is located in close proximity to the benzyl group of the first cation, the distance of the centroids of the aromatic groups being *ca.* 4.3 Å. This indicates offset face-to-face π···π interactions between them. The second disordered dication also complexes to resorcinarenes with both of its benzyl groups [Fig. 7(b) and 7(c)]. Due to the severe disorder of the cation, the DABCO moiety could not be unambiguously assigned for the second cation.

In complex **VII**, the asymmetric unit comprises one **1f**, half a $\mathbf{5}^{2+}$ and 2.5 EtOH molecules, and grows into a dimeric assembly of **1f** mediated by cation complexation to both resorcinarenes *via* its phenyl groups (Fig. 8). All of the EtOH molecules are disordered, making the study of hydrogen bonding difficult. Also, the DABCO moiety is severely disordered and it could not be unambiguously assigned from the electron density map. The phenyl groups interact with the aromatic groups of **1f** mostly face-to-face, the distance between the centroids of the interacting aromatic groups being 3.9 Å. Again the complex packs to form hydrophobic and hydrophilic layers throughout the crystal.

NMR titration studies

When resorcinarene **1b** was mixed with one of the guests $\mathbf{2}^{+}$, $\mathbf{4}^{2+}$ or $\mathbf{5}^{2+}$, significant complexation-induced upfield shifts of the guest signals were observed, as expected from the shielding effects of the aromatic rings of the bowl-shaped host cavity. This clearly points at fast guest exchange compared to the NMR time scale at room temperature and even down to 233 K. Job plot experiments[18] were performed in order to study the stoichiometry of the complexes (Fig. 9) and they indicate a clear 1 : 1 complexation model in methanol-d_4, irrespective of

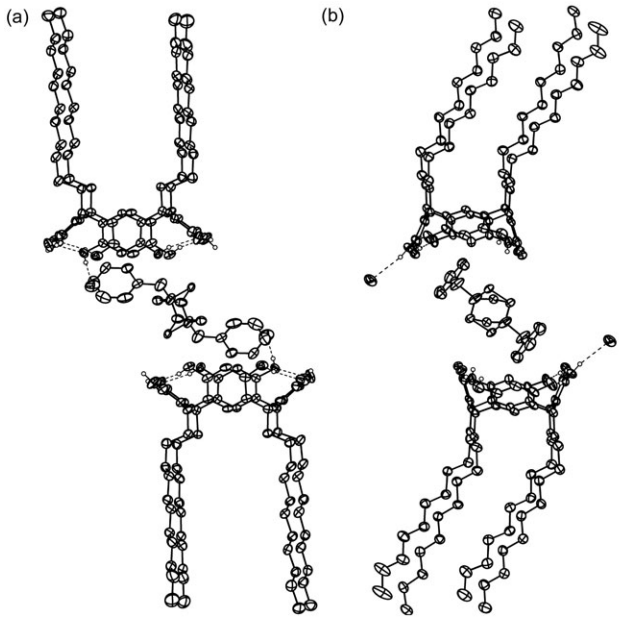

Fig. 8 Thermal ellipsoid plot of complex **VII** with 50% probability level. Solvents and non-hydrogen bonding hydrogens are omitted for clarity. (a) The 2 : 1 complex of **1d** and $\mathbf{5}^{2+}$. (b) View of the bending of the alkyl chains and the offset π···π interactions of $\mathbf{5}^{2+}$ benzyl groups with the interior of **1d** aromatic rings.

which of the guest signals was used for the evaluation of the experiment. The fact that 2 : 1 dimer formation is not observed, even in the case of tetramethyl ammonium $\mathbf{2}^{+}$, may be due to the efficiency with which the solvent competes with the hydrogen-bonding system and is included in the resorcinarene cavity, and that it also solvates quite well the ions present. Unfortunately, less polar solvents could not be used in the titration experiments due to the poor solubility of the corresponding salts in aprotic solvents.

Subsequently, ^{1}H NMR titrations of **1b** with the bromide salts of $\mathbf{2}^{+}$–$\mathbf{5}^{2+}$ were performed in the same solvent (*e.g.*, $\mathbf{4}^{2+}$ in Fig. 10). The binding constants for $\mathbf{2}^{+}$, $\mathbf{4}^{2+}$ and $\mathbf{5}^{2+}$ at 233 K were determined to be 460 ± 40, 570 ± 50 and 600 ± 45 M^{-1} by the least-squares global fitting of the titration curve with the Specfit program.[19] A model including only 1 : 1 complexes and free host and guest species was used, giving excellent fits, and thus confirming the Job plot analysis. The binding constants for singly and doubly charged guests are within a narrow range, with the binding of the dication being slightly stronger. Due to the small change in chemical shifts observed for the guest signals and overlapping solvent signals, the binding

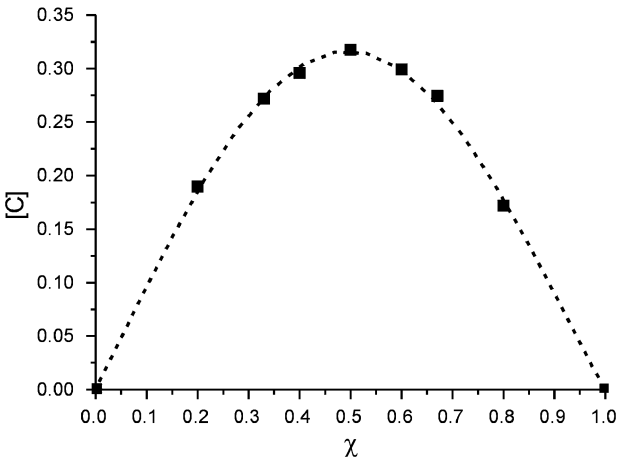

Fig. 9 Job plot of the complexation of $\mathbf{4}^{2+}$ by **1b**, as an example of a 1 : 1 complex stoichiometry.

View Article Online

Published on 09 December 2004 on http://pubs.rsc.org | doi:10.1039/B415401K
Downloaded on 01 January 2013

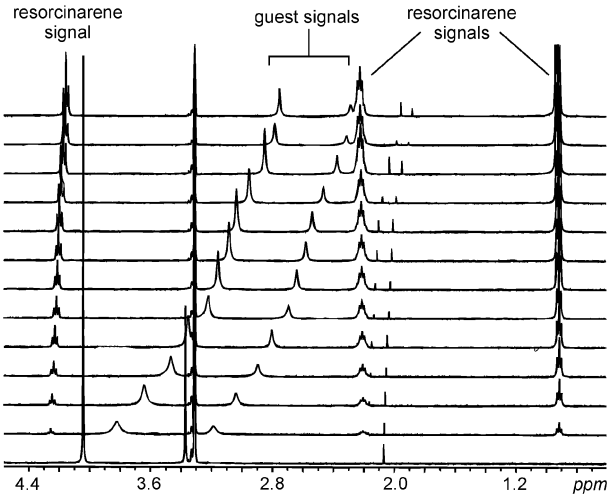

Fig. 10 ^{1}H NMR titration of $\mathbf{4}^{2+}$ with a solution of **1b** in methanol-d_4 at 233 K. At each step, 0.3 equiv. of a 60 mM resorcinarene solution were added to a 4 mM solution of $\mathbf{4}^{2+}(Br^-)_2$.

constant for $\mathbf{3}^{2+}$ could not be determined precisely. The binding constants for similar quaternary alkyl ammonium cations determined by Atwood and Szumna[10b] at 298 K [K_S = 93 M^{-1} for Me_4N^+ ($\mathbf{2}^+$), K_S = 81 M^{-1} for Et_4N^+ and K_S = 25 M^{-1} for Pr_4N^+] are in close agreement with our results.

In order to determine the enthalpic and entropic contributions to the binding of the cations inside the resorcinarene cavity, temperature-dependent measurements of the complexation constants of $\mathbf{2}^+$ and $\mathbf{4}^{2+}$ with **1b** were performed in the temperature range from 233 to 313 K (Table 1). Van't Hoff plots of ln*K versus* 1/*T* (Fig. 11) exhibit linear relationships for both $\mathbf{2}^+$ and $\mathbf{4}^{2+}$ cations, so that the separation of the enthalpic and entropic contributions to the binding is possible. The binding is largely enthalpic in nature with rather small binding entropies (ΔS). Both entropy values are slightly positive, although one might have expected negative values, since binding in a host-guest complex combines two molecules into one. However, solvation needs to be taken into account and methanol may well be present as a guest in the resorcinarene cavity[20] before addition of the ammonium cations. Consequently, expulsion of methanol from the cavity upon cation binding and removal of at least part of the solvation shell around the cation are plausible reasons for the slightly positive entropy.

In the NMR titrations of the bromide salt of $\mathbf{5}^{2+}$ with **1b**, complexation-induced chemical shifts were observed for both the central dicationic DABCO moiety as well as for the aromatic protons of the benzyl groups (Fig. 12). In view of the Job plots, this suggests that a mixture of two different 1 : 1 complexes is formed, which is in line with the solid state structures of complexes **VI** and **VII**, in which either the DABCO moiety is oriented into the resorcinarene cavity or one benzyl group is complexed in the cavity by π···π interactions, respectively. The binding constant can therefore only be regarded as the weighted average of those of the two complexes.

Finally, no complexation of any of the cations was observed in acetonitrile-d_3, likely due to the formation of acetonitrile

Table 1 Binding constants K_S at different temperatures and thermodynamic quantities for the interaction of **1b** with cations $\mathbf{2}^+$ and $\mathbf{4}^{2+}$

	K_S/M^{-1} at T/K				ΔH/kJ	ΔS/J
	233	258	288	313	mol^{-1}	mol^{-1} K^{-1}
$\mathbf{2}^+$	460 ± 40	340 ± 35	195 ± 35	110 ± 25	−10.7	6.0
$\mathbf{4}^{2+}$	570 ± 50	255 ± 30	145 ± 25	105 ± 30	−12.8	2.7

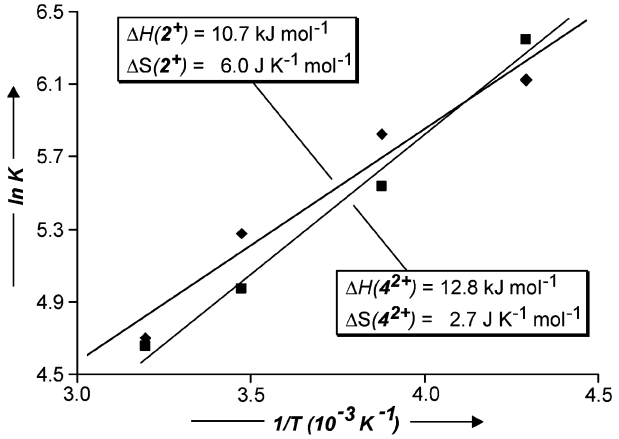

Fig. 11 Van't Hoff plot allowing to evaluate enthalpic and entropic contributions to the binding of ammonium ions $\mathbf{2}^+$ and $\mathbf{4}^{2+}$ with **1b**.

complexes with the resorcinarenes. Acetonitrile inclusion is common in calix[4]arene type cavities[17b,20] and competes with the complexation of the cations.

Mass spectrometric studies

Previously, we reported mass spectral studies of complexes of **1a** and **1b** with singly charged alkyl ammonium cations Me_4N^+ ($\mathbf{2}^+$), $Me_2Et_2N^+$, Et_4N^+ and Pr_4N^+, showing that dimeric molecular capsules of resorcinarene exist also in the gas phase, with the largest encapsulated guest being Et_4N^+.[6e] Similar experiments were conducted with doubly charged guests $\mathbf{3}^{2+}$–$\mathbf{5}^{2+}$. Since these guest cations are somewhat larger than tetramethyl ammonium, it is still an open question whether they would provide capsules detectable by mass spectrometry. In our previous studies in the crystalline state, two of the smallest of these guests, $\mathbf{3}^{2+}$ and $\mathbf{4}^{2+}$, were shown to form solvent-extended capsules similar to those containing singly charged guest ions in their cavity.[6e] In the gas phase, however, the capsules of singly charged cations are not solvent-mediated. In fact, we suspect the resorcinarenes in the Me_4N^+-containing capsules to be directly hydrogen-bonded to each other *via* the upper rim hydroxyl groups.

For electrospray ionization, solutions of the tetrafluoroborate salts of guests $\mathbf{3}^{2+}$–$\mathbf{5}^{2+}$ (50 μM) and the corresponding resorcinarenes were used. Doubly protonated DABCO $\mathbf{3}^{2+}$

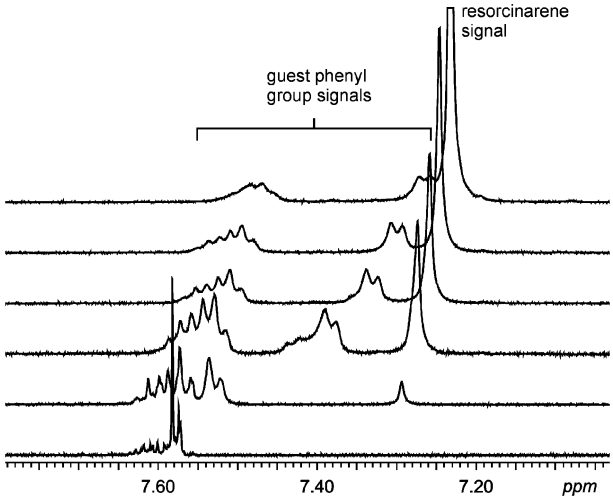

Fig. 12 The aromatic region of the ^{1}H NMR spectra of the titration of $\mathbf{5}^{2+}$ with a methanol-d_4 solution of **1b** at 233 K. The shift of the signals corresponding to the benzyl groups of the dication indicates binding interactions between the aromatics and the resorcinarene cavity.

View Article Online

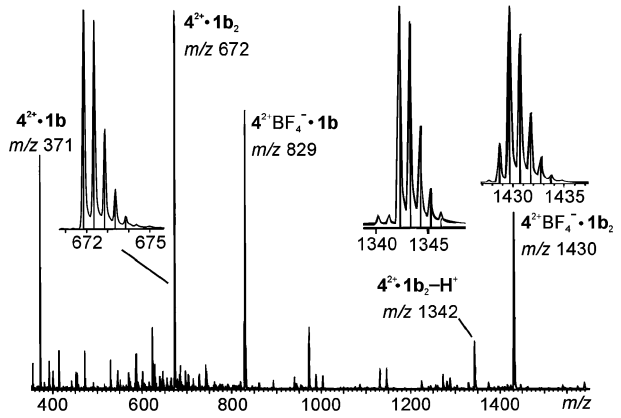

Fig. 13 Positive ion ESI mass spectrum of a mixture of $\mathbf{4}^{2+}BF_4^-$ and **1b** in acetonitrile. The insets show the experimental isotope patterns (curves) and those calculated on the basis of the natural abundance (line spectra), which agree well with each other. Note that the peak spacing is $\Delta m = 0.5$ amu for the signal at m/z 672, indicating a doubly charged ion.

turned out not to be the guest of choice for ESI-MS experiments, although it would have made comparison to the crystal structures and NMR data more straightforward. During the electrospray process, it loses one of the two protons and the major signals in the mass spectrum are due to complex formation with its singly protonated analogue. Only minor signals were observed for doubly charged complexes.

Consequently, we switched to the dimethylated DABCO $\mathbf{4}^{2+}$ as the guest cation (Fig. 13). In the spectrum of this guest with resorcinarene **1b**, the base peak corresponds indeed to the desired 1 : 2 complex of guest ion and resorcinarene $\mathbf{4}^{2+} \cdot \mathbf{1b}_2$ (m/z 672). This ion is doubly charged as evidenced by the spacings of $\Delta m = 0.5$ amu between two isotope peaks.

Besides two monomeric ions, that is, $\mathbf{4}^{2+} \cdot \mathbf{1b}$ (m/z 371) and $\mathbf{4}^{2+}BF_4^- \cdot \mathbf{1b}$ (m/z 829), two more singly charged dimeric complexes are formed. In the first, $\mathbf{4}^{2+} \cdot \mathbf{1b}_2\text{-}H^+$ (m/z 1342), one of the positive charges of the guest is compensated through deprotonation of one of the resorcinarene's OH groups. Since its elemental composition differs from that of $\mathbf{4}^{2+} \cdot \mathbf{1b}_2$ only by one hydrogen, the isotope pattern is basically the same, but the spacings between isotope peaks are now $\Delta m = 1$ amu, indicating the singly charged nature. The second singly charged dimer bears an additional BF_4^- anion and appears at m/z 1430. Since boron has two naturally occurring isotopes, ^{10}B and ^{11}B, the latter being the more abundant, the first signal in the isotope pattern is smaller than the second one. The ratio of these two indicates the presence of one boron atom and thus confirms that one anion is incorporated in the complex. Finally, a manifold of salt cluster signals, which we will not discuss in detail here, are observed at lower intensities. Resorcinarenes **1a** and **1c** behave quite similarly: the signals are just shifted according to the differences in mass for these derivatives.

Heterodimers again form quickly upon mixing solutions of **1a** and **1b** with $\mathbf{4}^{2+}(BF_4^-)_2$ as the guest salt. Fig. 14 depicts the region of the spectra in which the doubly charged dimer complexes $\mathbf{4}^{2+} \cdot \mathbf{1a}_2$ (m/z 616) and $\mathbf{4}^{2+} \cdot \mathbf{1b}_2$ (m/z 672) appear. Traces (a) and (b) in Fig. 14 correspond to the two solutions before mixing, and trace (c) shows the result after mixing. The two homodimers and the heterodimer form in almost exactly the expected statistical 1 : 2 : 1 ratio. The exchange of monomers is complete in less than a minute. It should be noted that, although not shown, the other dimeric complexes also give rise to heterodimers.

Also, the size selectivity was tested with bisbenzylated DABCO $\mathbf{5}^{2+}$, which is definitively too large to be trapped inside a dimeric capsule. Indeed, in the spectrum obtained from a competition experiment with $\mathbf{4}^{2+}$ and $\mathbf{5}^{2+}$, all signals correspond to complexes with $\mathbf{4}^{2+}$ as a subunit. In addition, mono-

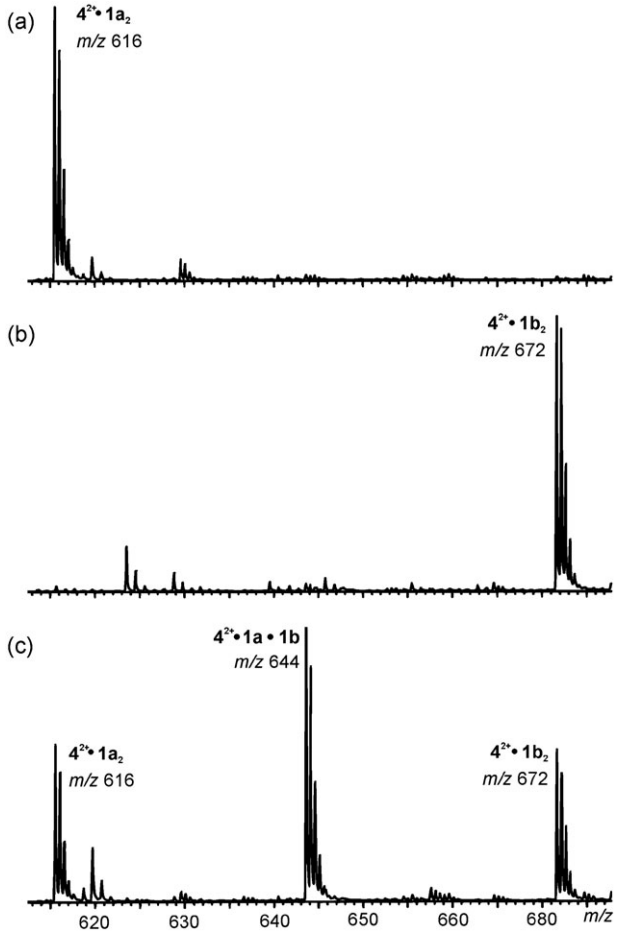

Fig. 14 Partial ESI mass spectra of: (a) $\mathbf{4}^{2+}BF_4^-$ with **1a**, (b) $\mathbf{4}^{2+}BF_4^-$ with **1b** and (c) $\mathbf{4}^{2+}BF_4^-$ with a 1 : 1 mixture of **1a** and **1b** in acetonitrile. Heterodimer formation is clearly observed in the statistical 1 : 2 : 1 ratio.

meric complexes with $\mathbf{5}^{2+}$ are also observed, but no signal could be detected for any dimeric complex with this cation.

We hoped that it would be possible to use in-source fragmentation of the dimeric capsules to gather some information on their structure, the same way as this was possible for the singly charged capsules discussed above. Unfortunately, these results were somewhat ambiguous. Upon increasing the sample cone voltage, the dimeric $\mathbf{4}^{2+} \cdot \mathbf{1b}_2$ ions vanished almost completely, indicating that these complexes do not represent very stable aggregates. However, HBF_4 is lost from $\mathbf{4}^{2+}BF_4^- \cdot \mathbf{1b}_2$ to generate $\mathbf{4}^{2+} \cdot \mathbf{1b}_2\text{-}H^+$, which gives an intense signal even at the highest possible sample cone voltage, while most of the other complexes were destroyed. Potentially, this suggests a much higher hydrogen bonding strength between a neutral and a singly deprotonated resorcinarene due to the charged nature of the $O\text{–}H\cdots O^-$ hydrogen bond. Here, the negative ion spectrum (Fig. 15) is more informative. In general, two different series of ions are observed: (i) resorcinarenes attach a single BF_4^- anion and yield $\mathbf{1b}_nBF_4^-$ complexes (n = 1–4) at m/z 687, 1287, 1887 and 2487, respectively; (ii) a second series is observed in which one doubly charged guest cation is bound together with two additional BF_4^- counterions. This gives rise to $\mathbf{4}^{2+} \cdot \mathbf{1b}_n(BF_4^-)_3$ complexes (n = 1–3) at m/z 1003, 1603 and 2203, respectively. From all these ions, loss of HBF_4 is possible, leading to ions containing a singly deprotonated resorcinarene (asterisks in Fig. 15). First of all, the complexes bearing three (and four) resorcinarene monomers are more prominent in this spectrum as compared to the positive ion spectrum, where they appeared with intensities hardly above the noise. They indicate that some unspecific aggregation occurs. However, at higher sample cone voltages they vanish

Published on 09 December 2004 on http://pubs.rsc.org | doi:10.1039/B415401K
Downloaded on 01 January 2013

Published on 09 December 2004 on http://pubs.rsc.org | doi:10.1039/B415401K
Downloaded on 01 January 2013

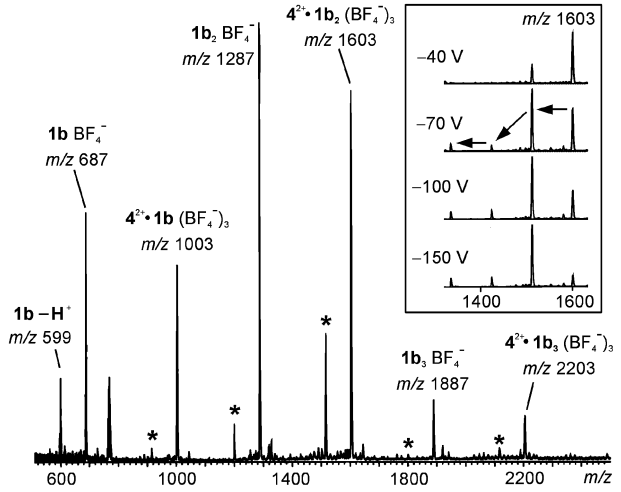

Fig. 15 Negative ion ESI mass spectrum of the acetonitrile solution mixture of $\mathbf{4}^{2+}BF_4^-$ and **1b**. Asterisks indicate HBF_4 loss related signals. The inset shows a series of spectra recorded at different sample cone voltages. At higher voltage, fragmentation is more pronounced and several consecutive HBF_4 losses are observed.

completely and can thus be destroyed easily. Most interestingly, the $\mathbf{4}^{2+} \cdot \mathbf{1b}_2(BF_4^-)_3$ ion at *m*/*z* 1603, upon increase of the sample cone voltage, shows three consecutive losses of HBF_4 rather than expulsion of the guest cation (inset in Fig. 15). The intensity of the signal at *m*/*z* 1603 decreases significantly in favour of that at *m*/*z* 1516 when collisions are induced by voltage changes. While no signal for additional losses of HBF_4 are observed at a sample cone voltage of −40 V, they appear at a voltage of −70 V and further increase somewhat, even when the voltage is increased to −150 V. The fact that the guest cation is still present in these complexes strongly indicates that it must be bound rather strongly and one reasonable explanation would be the formation of a capsule-like structure.

Consequently, the results for complexes containing doubly charged ammonium ions remain somewhat less convincing than those obtained for monocationic guests. Still, they point to the formation of capsules as far as size selectivity and fragmentation pattern for negatively charged species are concerned. The question remains though, on how a dimeric capsule, which has a preference for binding Me_4N^+ over Et_4N^+, [6e] could easily accommodate an even larger guest such as $\mathbf{4}^{2+}$. We suggest that the dication allows tighter binding due to its dicationic nature. Since each side of the dication may bind one resorcinarene with one charge, cation-π interactions will be stronger than those operative for the monocations. This would allow a higher packing coefficient, that is, the size of the guest relative to the empty cavity size, and thus, the formation of capsules would be possible despite the larger size of the guest cation. An impressive increase in packing coefficient from a standard 0.55 to 0.78, due to interactions of a cationic guest with a calixarene dimer has been reported previously.[13b,21] Similar effects would help to bind a larger, doubly charged guest inside a resorcinarene dimer. Another explanation would be that the seam of hydrogen bonds is not completely intact, when $\mathbf{4}^{2+}$ is encapsulated in $\mathbf{1b}_2$. An overall capsular structure would still be energetically not too unfavourable, because it may optimize the number of hydrogen bonds in combination with cation-π interactions with the guest cation. Such a structure, which is only close to a perfect capsule, would then also help to rationalize why the results obtained for the doubly charged guests speak somewhat less clearly in favour of a capsule.

AM1 semi-empirical calculations

Since the mass spectrometric results are somewhat ambiguous and different explanations may be invoked to rationalize them, we performed AM1 semi-empirical calculations of the resorcinarenes, their capsules, and their host–guest complexes with $\mathbf{2}^+$ and $\mathbf{4}^{2+}$ in the gas phase in order to get an idea of the structures of the ions involved. These calculations should also clarify whether a fully closed capsule of two resorcinarenes is possible, even in the absence of solvent molecules and counterions, when any of the ammonium cations included in this study is inside the cavity. The binding of the cations inside a capsule involves cation-π interactions, which rules out most force fields for molecular modelling, because they usually do not include the necessary parameters to describe these interactions reasonably. Indeed, some preliminary tests with several of them immediately showed that they did not give results consistent with the experimental data.

Fig. 16 shows the optimized structures of the empty monomer and dimer of **1a** and their complexes with tetramethyl ammonium $\mathbf{2}^+$. The resorcinarenes are held in a crown conformation through intramolecular hydrogen bonding. The empty dimer shows a capsular structure in which the aromatic rings of the two resorcinarenes adopt a staggered conformation. The eclipsed arrangement, which has been found in the crystal structures of several solvent-mediated capsules,[6e] suffers from steric repulsion of the aromatic hydrogen atoms located between the resorcinarene OH groups on each aromatic ring. Eight O–H···O hydrogen bonds connect the two halves of the dimer. The calculated binding energy for the empty dimeric capsule amounts to *ca.* 88 kJ mol^{-1}. This value (as most others included here) seems to be quite high, but if one considers that

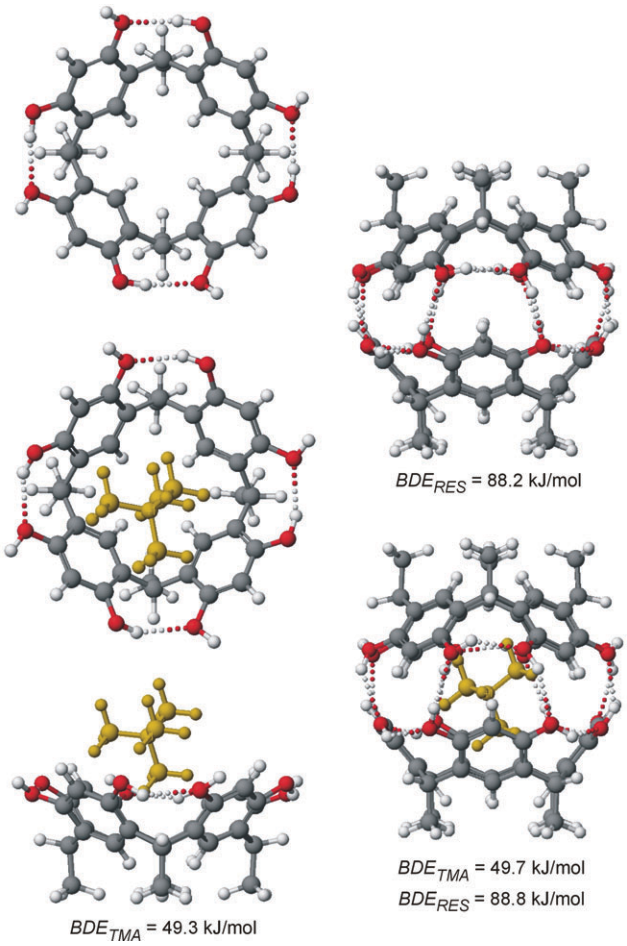

Fig. 16 AM1-optimized geometries of the resorcinarene monomer **1a** in its crown conformation (top left), its empty dimer (top right), the monomeric $\mathbf{2}^+ \cdot \mathbf{1a}$ complex (bottom left, shown as top and side views), and the dimer-guest complex $\mathbf{2}^+ \cdot \mathbf{1a}_2$ (bottom right). Hydrogen bonds are shown as dotted lines. The bond dissociation energies represent the calculated binding energies of the tetramethyl ammonium cation (BDE_{TMA}) and of the two resorcinarene monomers (BDE_{RES}).

View Article Online

the calculations represent gas-phase structures, which do not suffer from competing solvent molecules, the energies appear to be reasonable. In methanol solution, this binding energy is likely reduced to almost zero and thus, binding of two resorcinarenes is not observed in the NMR experiments. However, empty dimers can be clearly detected in the gas phase as protonated species, when sprayed from methanol. The binding energy of the cation to the resorcinarene monomer is *ca.* 49 kJ mol^{-1}. The cation is almost exactly centred inside the cavity with one methyl group pointing into the resorcinarene bowl.

The most favourable cation-dimer complex $\mathbf{2}^+ \cdot \mathbf{1a}$ corresponds to a closed capsule, whose geometry and hydrogen-bonding pattern do not change significantly with respect to the empty capsule. For the small tetramethyl ammonium cation, formation of a capsule without solvent molecules mediating the hydrogen-bonding seam is thus possible, which is in good agreement with the mass spectral data published previously.[6e] It is quite interesting to see that none of the binding energies discussed above changes much when the inclusion complex is compared to the monomer-guest complex or the empty capsule. The examination of the binding of dication $\mathbf{4}^{2+}$ requires first to consider different orientations of the guest inside the host. Three different monomer-guest complexes $\mathbf{4}^{2+} \cdot \mathbf{1a}$ are shown in Fig. 17. It turns out that an arrangement corresponding to an orientation of $\mathbf{2}^+$ in which one methyl group points into the resorcinarene bowl does not correspond to the most energetically favourable structure. Instead, the insertion of one CH_2CH_2 bridge of the dication is optimal, because (i) it maximizes electrostatic interactions of the cation with the partially negative oxygen atoms by minimizing the distance and (ii) the four hydrogen atoms from the bridge inside the cavity can favourably interact with the four aromatic rings of the resorcinarene. They are almost perfectly arranged on top of the four rings and thus, correspond much better to the fourfold symmetry of the host than a methyl group. Consequently, CH-π interactions can contribute significantly to the stability of the complex. This arrangement is found in many of the crystal structures of resorcinarenes with $\mathbf{4}^{2+}$ (Figs. 2, 5 and 6). The dication in its upright arrangement is also found, although the calculations predict it to be energetically less favourable. This may be due to the counterions being close to the dication in these structures (Figs. 3 and 4). The calculations are thus in excellent agreement with our experimental results.

When $\mathbf{4}^{2+}$ was inserted into the closed capsule of the resorcinarene dimer shown in Fig. 16, the calculation optimized to two conformers for $\mathbf{4}^{2+} \cdot \mathbf{1a}_2$, which differ by the orientation of the dication (Fig. 17, bottom). Obviously, the dication is too large to fit inside a fully closed capsule without solvent participation and part of the hydrogen bonding seam is thus broken. In both structures, three hydrogen bonds connecting the two halves remain. Such structures are in line with the results obtained by mass spectrometry.

The binding energy of one resorcinarene monomer to the monomeric host–guest complex is higher than that calculated for the empty dimer shown in Fig. 16, although the seam of hydrogen bonds is not intact in $\mathbf{4}^{2+} \cdot \mathbf{1a}_2$. This suggests that a significant part of the binding energy comes from the interaction with the dicationic guest rather than the other resorcinarene monomer. Similarly, a more than three times higher binding energy is calculated for the monomer-guest complex $\mathbf{4}^{2+} \cdot \mathbf{1a}$ compared to the monocationic analogue $\mathbf{2}^+ \cdot \mathbf{1a}$. Apparently, the horizontal orientation of the dication provides quite a significant optimization of the binding interactions, compared to the situation where a methyl group is diving into the cavity.

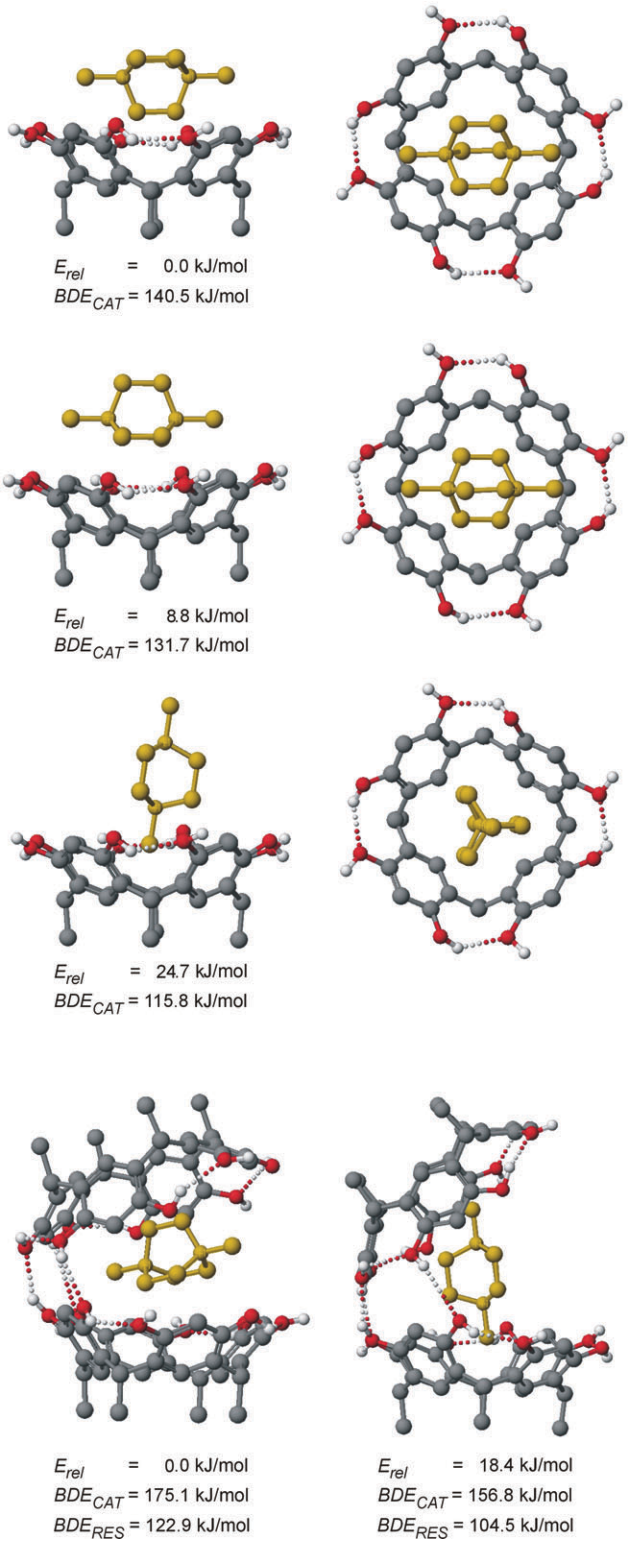

Fig. 17 From top to bottom: three AM1-optimized geometries of different conformations of $\mathbf{4}^{2+} \cdot \mathbf{1a}$ shown as side (left) and top (right) views, which differ from each other only with respect to the orientation of the encapsulated dication, and AM1-optimized structures (left and right, bottom) of two conformations of the dimer-guest complex $\mathbf{4}^{2+} \cdot \mathbf{1a}_2$. E_{rel} provides the calculated relative stability of the structures, BDE_{CAT} refers to the calculated binding energies of the dication, and BDE_{RES} refers to the dication binding energies relative to the empty dimer shown in Fig. 16. Hydrogen bonds shorter than 3.5 Å are shown as dotted lines. It should be noted that relative energies can only be compared within a series of species with the same elemental formula.

Conclusions

The present paper collects structural information on host–guest complexes of alkyl ammonium ions and resorcinarenes: in the solid state, where packing and space filling is an important factor; in solution, where interactions with solvents come into play; in the gas phase, where no environment is

Published on 09 December 2004 on http://pubs.rsc.org | doi:10.1039/B415401K
Downloaded on 01 January 2013

View Article Online

Table 2 Crystal data and collection parameters

	I	II	III	IV	V	VI	VII
	1e · 0.5 $\mathbf{2}^{2+}$ · 0.5 Br^- · 2.5 MeOH · 0.5 H_2O	**1b** · 2 $\mathbf{4}^{2+}$ · 4 Br^- · *n*-PrOH · 2 H_2O	**1b** · $\mathbf{4}^{2+}$ · 2 Br^- · EtOH	**1c** · $\mathbf{4}^{2+}$ · 2 Cl^- · 2 MeOH	**1d** · 1.5 $\mathbf{4}^{2+}$ · 3 Br^- · EtOH · H_2O	2 **1c** · 1.5 $\mathbf{5}^{2+}$ · 3 Br^- · 0.5 H_2O · 7 MeOH	**1f** · 0.5 $\mathbf{5}^{2+}$ · Br^- · 2.5 EtOH
Formula	$C_{64.5}H_{73}O_{11}N_{0.5}Br_{0.5}$	$C_{55}H_{88}O_{11}N_4Br_4$	$C_{46}H_{64}O_9N_2Br_2$	$C_{50}H_{74}O_{10}N_2Cl_2$	$C_{66}H_{107}O_{10}N_3Br_3$	$C_{117}H_{164}O_{23.5}N_3Br_3$	$C_{87}H_{140}O_{10.5}NBr$
M_r	2142.4	1300.9	948.8	934.0	1342.3	2228.2	1447.9
a/Å	29.4551(5)	12.4513(2)	12.0544(1)	11.3877(2)	53.2560(8)	15.8558(3)	9.8246(1)
b/Å	15.4086(2)	13.6703(2)	12.8536(2)	12.5699(3)	12.6490(3)	17.8230(4)	15.7155(2)
c/Å	25.4790(5)	19.7836(4)	15.3163(2)	17.5983(4)	20.5761(7)	20.2560(4)	26.8439(4)
α/°	90	71.716(5)	85.953(1)	99.359(1)	90	85.693(1)	91.387(1)
β/°	99.503(3)	79.631(5)	84.491(1)	91.183(1)	97.955(1)	88.540(1)	91.438(1)
γ/°	90	72.394(1)	69.520(1)	98.780(1)	90	86.632(1)	92.686(1)
U/Å^3	11405.3(3)	3034.2(1)	2211.1(1)	2453.7(1)	13727.4(6)	5697.0(2)	4137.5(1)
Z	8	2	2	2	4	2	2
Space system	Monoclinic	Triclinic	Triclinic	Triclinic	Monoclinic	Triclinic	Triclinic
Space group	*C*2/*c* (no. 15)	*P*-1 (no. 2)	*P*-1 (no. 2)	*P*-1 (no. 2)	*C*2/*c* (no. 15)	*P*-1 (no. 2)	*P*-1 (no. 2)
ρ_{calcd}/Mg m^{-3}	1.248	1.424	1.425	1.264	1.299	1.299	1.162
μ/mm^{-1}	0.432	2.71	1.890	0.191	1.818	1.133	0.553
Reflections measured	17408	24116	22107	13446	32427	32249	21336
Unique reflections	10066	10107	8301	8605	11413	17331	14265
Reflections used in refinement[a]	5632	6452	7209	5747	3703	8271	9062
R_{int}	0.058	0.046	0.029	0.035	0.137	0.094	0.032
R	0.108	0.049	0.030	0.061	0.068	0.074	0.063
wR	0.276	0.077	0.065	0.128	0.134	0.139	0.118

[a] With $I > 2\sigma(I_0)$.

Published on 09 December 2004 on http://pubs.rsc.org | doi:10.1039/B415401K
Downloaded on 01 January 2013

present at all; and complements them with semi-empirical calculations.

When small quaternary cations are complexed by resorcinarenes, solvent-mediated dimeric capsules are formed quite often in the solid state, while such capsules are stable in the gas phase even without solvent connecting the hydrogen-bonding seams.[6e] The use of a polar competitive solvent such as methanol or acetonitrile destroys these capsules in solution in favour of either 1 : 1 complexes or resorcinarenes occupied solely by solvent molecules.

The use of the larger, doubly charged *N*,*N*′-bisalkylated DABCO derivatives prevents, in most cases, the formation of a fully closed capsule. In the crystal, 1 : 1 complexes are co-crystallized, while capsules are scarcely found,[6f] and in solution, only 1 : 1 complexes are formed. In the mass spectra, however, signals appear for 2 : 1 complexes, which very likely do not have a capsular structure, but rather incorporate the cation in a "half-open capsule". Part of the seam of hydrogen bonds remains intact and the interactions with the dicationic guests are maximized in such structures. In terms of energies, the situation in the gas phase differs radically from that in methanol solution. In the gas phase, no competition of the hydrogen bonds between two resorcinarenes with those formed with methanol occurs.

The counterions play a significant role in each of the solid state structures as hydrogen bond acceptors and only complexes of alkyl ammonium halide salts have successfully been crystallized, while salts with poor H-bond acceptors, such as BF_4 and PF_6, have resulted as precipitates or crystals of the starting compounds. In solution, the counterions stabilize the cations and thus diminish the binding energies significantly, while methanol, as a good hydrogen-bond donor and acceptor, interferes with the binding of the two resorcinarenes. In the gas phase, the counterions are absent and thus the intrinsic binding energies fully support the formation of 2 : 1 complexes of resorcinarenes, even with larger guests, which destroy part of the seam of hydrogen bonds.

In view of earlier reports,[6,10] which showed additional effects coming from the counterions or the length of the resorcinarene side chain, we are now able to conclude that resorcinarenes, although quite rigid, offer a rich structural chemistry full of subtleties, which depend on the details of their particular features as well as on the properties of their environment.

The differences in behaviour in all three states makes it difficult to draw conclusions from, for example, an X-ray crystal structure and extrapolate to the properties in solution. On the other hand, the amount of information on noncovalent forces gathered from these systems is particularly high because of these differences, which provide more insight into the role of the environment than many other systems. Understanding these subtle effects certainly contributes to obtaining significant insight into noncovalent interactions, which are important in many other fields of chemistry.

Experimental

Crystal structure determination

The solid state structures were crystallized by slow evaporation of the solvent from 2 : 1 mixtures of the corresponding resorcinarenes and alkylammonium salts in aqueous MeOH, EtOH or *n*-propanol. In all cases the crystals formed within one week. A selection of crystal data and collection parameters are compiled in Table 2.†

The X-ray crystallographic data for all complexes were recorded with a Nonius Kappa CCD diffractometer. Graphite monochromated MoKα radiation ($\lambda_{MoK\alpha}$ = 0.710 73 Å) and a temperature of 173.0 ± 0.1 K were used in all cases. The CCD data were processed with Denzo-SMN v. 0.95.373 [22a] and all structures were solved by direct methods (SHELXS-97 [22b]) and refined on F^2 by full-matrix least-squares techniques

† CCDC reference numbers 254958–254964. See http://www.rsc.org/suppdata/nj/b4/b415401k/ for crystallographic data in .cif or other electronic format.

View Article Online

(SHELXL-97 [22c]). Whenever possible, the hydrogen atoms of the resorcinarene groups were located from the electron density map and the rest of the hydrogen atoms were calculated in their idealized positions with isotropic temperature factors (1.2 or 1.5 times the carbon temperature factor) and refined as riding atoms. The MeOH molecule and the cation in complex **I**, one EtOH molecule in **V**, one of the cations in **VI** and one EtOH molecule in **VII** were disordered and treated isotropically, while the disordered Br^- and H_2O in complex **I**, the ethyl group of **1b** in **II**, the hexyl group of **1d**, the $Br^-$and H_2O in **V**, the Br^- in **VI** and the EtOH molecule and cation in **VII** could all be treated anisotropically, despite the disorder.

^{1}H NMR titration

NMR titrations were performed in methanol-d_4 by titrating 1 ml of a 4 mM solution of the bromide salt of the corresponding alkyl ammonium salt with a 60 mM solution of ethyl resorcin[4]arene. The ^{1}H NMR spectra of each titration step was measured on a 500 MHz Bruker Avance DRX spectrometer equipped with temperature regulation. Binding constants were obtained by fitting the titration curves with the Specfit program package.[19]

ESI-TOF mass spectroscopy

The mass spectrometric experiments were performed with a Micromass LCT ESI-TOF instrument equipped with a Z geometry electrospray ion source. For both positive and negative ion spectra, the samples were introduced into the source as acetonitrile solution mixtures of **1a** (50 μM) and the salts of doubly charged cations $\mathbf{4}^{2+}$ and $\mathbf{5}^{2+}$ (50 μM) at flow rates of 15 μl min^{-1}. Tetrafluoroborate salts of these guests gave the best results, probably due to increased solubility in acetonitrile, but bromides could also be used. Acetone was an alternative spray solvent and gave almost identical results. The addition of methanol is not advantageous, but a minor amount might help to dissolve the salts without hampering the measurements.

Constant spray and highest intensities were achieved with a capillary voltage of 3700 V at a source temperature of 80 °C and a dissolvation temperature of 120 °C. Other selected source parameters were as follows: sample cone voltage 20–30 V; extraction cone voltage 3–6 V; flow of cone gas 10 l h^{-1}; flow of dissolvation gas 150 l h^{-1}. Other parameters did not influence much the ion intensities. The sample cone voltage was optimum at a somewhat higher value of 50 V for negative ion spectra. For the examination of heterodimer formation, two of the sample solutions were mixed in a 1 : 1 ratio and then subjected to the same experiments. Multiple scans (50–200) were recorded and averaged for each spectrum in order to improve the signal-to-noise ratio. Since the instrument does not permit MS/MS experiments, the fragmentation behaviour of the samples was examined by in-source fragmentation, induced by collisions with the gas molecules present in the ion source. For this purpose, the ions were accelerated to different kinetic energies by varying the sample cone voltage. At high voltages, the ions undergo collisions at higher velocities and usually pronounced fragmentation is observed.

AM1 calculation

Several alternative conformations of the molecules and complexes shown in Fig. 16 and Fig. 17 were optimized at the AM1 level of theory[23] as implemented in the MOPAC version delivered with the CaChe 5.0 program package.[24]

Published on 09 December 2004 on http://pubs.rsc.org | doi:10.1039/B415401K
Downloaded on 01 January 2013

Acknowledgements

The Graduate School of Bio-organic and Medicinal Chemistry (H.M.) and Academy of Finland (M.N.) are gratefully acknowledged. C.A.S. wishes to thank the Deutsche Forschungsgemeinschaft for a Heisenberg fellowship, the Fonds der Chemischen Industrie for a Dozentenstipendium, and the Deutscher Akademischer Austauschdienst for travel support. We also wish to thank Mr Reijo Kauppinen and Prof. Erkki Kolehmainen for assistance with the NMR experiments and Dr Minna Luostarinen for providing the resorcinarenes.

References

1 (*a*) M. M. Conn and J. Rebek, Jr., *Chem. Rev.*, 1997, **97**, 1647; (*b*) C. A. Schalley, *Adv. Mater.*, 1999, **11**, 1535; (*c*) J. Rebek, Jr., *Acc. Chem. Res.*, 1999, **32**, 278; (*d*) C. A. Schalley and J. Rebek, Jr., in *Chemical Encapsulation in Self-Assembling Capsules, Stimulating Concepts in Chemistry*, eds. J. F. Stoddart, F. Vögtle and M. Shibasaki, Wiley–VCH, Weinheim, 2000, p. 199.
2 T. Heinz, D. M. Rudkevich and J. Rebek, Jr., *Nature (London)*, 1998, **394**, 764.
3 (*a*) J. M. Rivera, T. Martín and J. Rebek, Jr., *Science*, 1998, **279**, 1021; (*b*) R. K. Castellano, C. Nuckolls and J. Rebek, Jr., *J. Am. Chem. Soc.*, 1999, **121**, 11156.
4 (*a*) J. Kang and J. Rebek, Jr., *Nature (London)*, 1997, **385**, 50; (*b*) J. Kang, J. Santamaría, G. Hilmersson and J. Rebek, Jr., *J. Am. Chem. Soc.*, 1998, **120**, 7389.
5 K. Murayama and K. Aoki, *Chem. Commun.*, 1997, 119.
6 (*a*) K. Murayama and K. Aoki, *Chem. Commun.*, 1998, 607; (*b*) K. N. Rose, L. J. Barbour, G. W. Orr and J. Atwood, *Chem. Commun.*, 1998, 407; (*c*) A. Shivanyuk, K. Rissanen and E. Kolehmainen, *Chem. Commun.*, 2000, 1107; (*d*) A. Shivanyuk and J. Rebek, Jr., *Chem. Commun.*, 2001, 2374; (*e*) H. Mansikkamäki, M. Nissinen and C. A. Schalley, *New. J. Chem.*, 2003, **27**, 88; (*f*) H. Mansikkamäki, M. Nissinen and K. Rissanen, *Chem. Commun.*, 2002, 1902.
7 (*a*) G. W. Orr, L. J. Barbour and J. L. Atwood, *Science*, 1999, **285**, 1049; (*b*) H. Mansikkamäki, M. Nissinen and K. Rissanen, *Angew. Chem., Int. Ed.*, 2004, **43**, 1243.
8 L. R. MacGillvray and J. L. Atwood, *Nature (London)*, 1997, **389**, 469.
9 (*a*) A. Shivanyuk and J. Rebek, Jr., *Chem. Commun.*, 2001, 2424; (*b*) A. Shivanyuk and J. Rebek, Jr., *Proc. Natl. Acad. Sci. USA*, 2001, **98**, 7662; (*c*) L. Avram and Y. Cohen, *Org. Lett.*, 2002, **4**, 4365; (*d*) L. Avram and Y. Cohen, *J. Am. Chem. Soc.*, 2002, **124**, 15148; (*e*) A. Shivanyuk and J. Rebek, Jr., *J. Am. Chem. Soc.*, 2002, **4**, 3433; (*f*) A. Schivanyuk and J. Rebek, Jr., *J. Am. Chem. Soc.*, 2003, **125**, 3432.
10 For earlier NMR studies on interactions of resorcinarenes with alkyl ammonium cations, see: (*a*) H. J. Schneider, D. Güttes and U. Schneider, *Angew. Chem., Int. Ed. Engl.*, 1986, **25**, 647; (*b*) J. L. Atwood and A. Szumna, *J. Supramol. Chem.*, 2002, **2**, 479.
11 J. C. Ma and D. A. Dougherty, *Chem. Rev.*, 1997, **97**, 1303.
12 (*a*) M. Przybylski and M. O. Glocker, *Angew. Chem., Int. Ed. Engl.*, 1996, **35**, 806; (*b*) J. S. Brodbelt, *Int. J. Mass Spectrom.*, 2000, **200**, 57; (*c*) C. A. Schalley, *Int. J. Mass Spectrom.*, 2000, **194**, 11; (*d*) C. B. Lebrilla, *Acc. Chem. Res.*, 2001, **34**, 653; (*e*) C. A. Schalley, *Mass Spectrom. Rev.*, 2001, **20**, 253.
13 (*a*) C. A. Schalley, J. M. Rivera, T. Martín, J. Santamaría, G. Siuzdak and J. Rebek, Jr., *Eur. J. Org. Chem.*, 1999, 1325; (*b*) C. A. Schalley, R. K. Castellano, M. S. Brody, D. M. Rudkevich, G. Siuzdak and J. Rebek, Jr., *J. Am. Chem. Soc.*, 1999, **121**, 4568; (*c*) M. S. Brody, D. M. Rudkevich, C. A. Schalley and J. Rebek, Jr., *Angew. Chem., Int. Ed.*, 1999, **38**, 1640; (*d*) C. A. Schalley, T. Martín, U. Obst and J. Rebek, Jr., *J. Am. Chem. Soc.*, 1999, **121**, 2133; (*e*) A. Lützen, A. R. Renslo, C. A. Schalley, B. M. O'Leary and J. Rebek, Jr., *J. Am. Chem. Soc.*, 1999, **121**, 7455; (*f*) B. M. O'Leary, T. Szabo, N. Svenstrup, C. A. Schalley, A. Lützen and J. Rebek, Jr., *J. Am. Chem. Soc.*, 2001, **123**, 11519.
14 (*a*) J. A. Bryant, M. T. Blanda, M. Vincenti and D. J. Cram, *J. Am. Chem. Soc.*, 1991, **113**, 2167; (*b*) L. M. Nuwaysir, J. A. Castoro, C. L.-C. Yang and C. L. Wilkins, *J. Am. Chem. Soc.*, 1992, **114**, 5748; (*c*) F. Inokuchi, Y. Miyahara, T. Inazu and S. Shinkai, *Angew. Chem.*, 1994, **34**, 1364; (*d*) P. S. H. Wong, X. Yu and D. V. Dearden, *Inorg. Chim. Acta*, 1996, **246**, 259; (*e*) E. Ventola, K. Rissanen and P. Vainiotalo, *Chem. Commun.*, 2002, 1110; (*f*) M. Mäkinen, P. Vainiotalo and K. Rissanen, *J. Am. Soc.*

View Article Online

Mass Spectrom., 2002, **7**, 851; (*g*) M. Mäkinen, M. Nissinen, K. Rissanen and P. Vainiotalo, *J. Am. Chem. Soc.*, 2003, **14**, 143; (*h*) M. C. Letzel, B. Decker, A. B. Rozhenko, W. W. Schoeller and J. Mattay, *J. Am. Chem. Soc.*, 2004, **126**, 9669.

15 (*a*) L. R. MacGillivray and J. Atwood, *J. Am. Chem. Soc.*, 1997, **119**, 6931; (*b*) L. R. MacGillivray, G. S. Papaefstathiou, J. L. Reid and J. A. Ripmeester, *Cryst. Growth Des.*, 2001, **1**, 373; (*c*) B.-Q. Ma and P. Coppens, *Chem. Commun.*, 2003, **504**; (*d*) I. Gregoriev and E. Bosch, *Cryst. Growth Des.*, 2004, **4**, 235.

16 D. E. Hibbs, M. B. Hursthouse, K. M. A. Malik, H. Adams, C. J. M. Stirling and F. Davis, *Acta Crystallogr., Sect. C*, 1996, **54**, 987.

17 (*a*) W. Iwanek, R. Frölich, M. Urbaniak, C. Näther and J. Mattay, *Tetrahedron*, 1998, **54**, 14031; (*b*) M. Nissinen and K. Rissanen, *Supramol. Chem.*, 2003, **15**, 581.

18 (*a*) K. A. Connors, *Binding Constants*, Wiley, New York, 1987; (*b*) K. Hirose, *J. Inclusion Phenom. Macrocycl. Chem.*, 2001, **39**, 193 and references cited therein.

19 *Specfit*, version3.0.31, Spectrum Software Associates, Chapel Hill, NC, USA, 2002. See also: H. Gampp, M. Maeder, C. J. Meyer and A. D. Zuberbühler, *Talanta*, 1986, **33**, 943 and references cited therein.

20 J. C. Shivanyuk, S. Friese, S. Döring and J. Rebek, Jr., *J. Org. Chem.*, 2003, **68**, 6489.

21 This has been confirmed by a crystal structure, see: I. Thondorf, F. Broda, K. Rissanen, M. Vysotsky and V. Böhmer, *J. Chem. Soc., Perkin Trans. 2*, 2002, 1796.

22 References to programs used for crystallographic work: (*a*) Z. Otwinowski and W. Minor, Processing of X-ray Diffraction Data Collected in Oscillation Mode, in *Methods in Enzymology, Macromolecular Chrystallography, Part A*, eds. C. W. Carter, Jr. and R. M. Sweet, Academic Press, New York, 1997, vol. **276**, p. 307; (*b*) G. M. Sheldrick, *SHELXS-97, Program for solution of crystal structures*, University of Göttingen, Germany, 1997; (*c*) G. M. Sheldrick, *SHELXL-97, Program for refinement of crystal structures*, University of Göttingen, Germany, 1997.

23 M. J. S. Dewar, E. G. Zoebisch, E. F. Healy and J. J. P. Stewart, *J. Am. Chem. Soc.*, 1985, **107**, 3902.

24 *CACHE 5.0 for Windows*, Fujitsu Ltd., Krakow, Poland, 2001.

Published on 09 December 2004 on http://pubs.rsc.org | doi:10.1039/B415401K
Downloaded on 01 January 2013